

## Investigation of morphological features and thermal stability of regenerated wood cellulose from solutions in [BMIm]Cl

Mariya G. Mikhaleva<sup>1,a</sup>, Sergey V. Usachev<sup>1,b</sup>, Alexander S. Vedenkin<sup>1,2,c</sup>, Mariya I. Ikim<sup>1,d</sup>, Galina G. Politenkova<sup>1,e</sup>, Sergey M. Lomakin<sup>2,f</sup>

<sup>1</sup>N.N. Semenov Federal Research Center for Chemical Physics, Russian Academy of Sciences, Moscow, Russia

<sup>2</sup>Emanuel Institute of Biochemical Physics, Russian Academy of Sciences, Moscow, Russia

<sup>a</sup>maria.mikhaleva@chph.ras.ru, <sup>b</sup>usachevsv@inbox.ru, <sup>c</sup>alexander.vedenkin@chph.ras.ru,

<sup>d</sup>maria.ikim@chph.ras.ru, <sup>e</sup>galina.politenkova@chph.ras.ru, <sup>f</sup>lomakin@sky.chph.ras.ru

Corresponding author: Mariya G. Mikhaleva, maria.mikhaleva@chph.ras.ru

PACS 61.25.Hq

**ABSTRACT** A study of the morphological features of regenerated wood pulp LS-0 obtained from its solutions in [BMIm]Cl at concentrations ranging from 2 to 26 % has been performed. It was demonstrated that at concentrations of LS-0 up to 8 % in [BMIm]Cl, thermograms exhibited a reduction in thermal stability concomitant with an increase in coke residue. In samples of regenerated cellulose obtained from solutions with an LS-0 content of 14 % or more, two maxima are observed on the differential thermogravimetric curves (DTG). This phenomenon was explained by the presence of two phases formed during the dissolution-regeneration process. The impact of [BMIm]Cl on the structural characteristics of regenerated cellulose was investigated through IR spectroscopy and X-ray diffraction analysis.

**KEYWORDS** cellulose, ionic liquids, thermogravimetry, infrared spectroscopy, X-ray structural analysis

**ACKNOWLEDGEMENTS** The study was conducted under the state assignment of the Federal Research Center for Chemical Physics of the Russian Academy of Sciences.

**FOR CITATION** Mikhaleva M.G., Usachev S.V., Vedenkin A.S., Ikim M.I.M., Politenkova G.G., Lomakin S.M. Investigation of morphological features and thermal stability of regenerated wood cellulose from solutions in [BMIm]Cl. *Nanosystems: Phys. Chem. Math.*, 2025, **16** (3), 364–373.

### 1. Introduction

Cellulose, a renewable natural polymer, has long been the subject of considerable interest, both in terms of its potential applications in various spheres of human life and the study of its physicochemical properties [1–3]. The unique structure of cellulose is a combination of amorphous and crystalline particles that together determine its properties [4]. The fundamental monomeric unit is typically regarded as a cellobiose, which unites two glucose residues through a  $\beta$ -glycosidic bond [5]. In contrast to the typical  $\alpha$ -glycosidic linkages of starch, these linkages are more resistant to acid hydrolysis. The strength of the cellulose polymer chain is due to hydrogen bonds between hydroxyl groups included in cellobiose [6,7]. Interactions between adjacent chains lead to the formation of structural fragments – fibrils, which have an ordered structure and form microcrystalline regions [4]. This structure of cellulose determines its properties on the macro level. Depending on their origin, cellulose fibers have different degrees of polymerization (DP), which determine their field of application. Flax fibers have the greatest length [8], which allows them to be used in the production of ropes and in the textile industry. Cotton fibers have a lower DP and are primarily used in the textile industry. Wood cellulose, which is the most common, has a DP of 103 – 104 and is mainly used in paper production. Since cellulose does not allow direct processing, the chemical modification of its glycosidic units by the formation of ether groups has been used to expand the range of its applications [8]. This modification affects the hydroxyl groups of both amorphous and crystalline regions of cellulose. Based on this process, nitrocellulose [10], cellulose sulfite and acetate [11] were obtained. When cellulose is dissolved in Schweitzer's reagent (copper ammine) [12], spinning solutions are formed. When they are extruded into acidified water, free hydrated cellulose is formed. The dissolution of cellulose without its chemical modification has been demonstrated using dimethylacetamide with lithium chloride [13, 14], in aqueous solutions of transition metal complexes with amines, molten hydrates of inorganic salts [15], and various quaternary ammonium salts in DMSO [16, 17]. Other studies have used ionic liquids in DMSO [18] or N-methylimidazole [19], as well as a combination of the ionic liquid [BMIm]OAc with LiCl [14]. The use of mono-solvents allows them to be used in recycling. An illustrative example is N-methylmorpholin oxide (NMO), which was proposed in 1939 [20]. This compound was subsequently employed in the production of Liocell fibers. In this process, NMO is reused following its extraction from the wash water. Another group

of monosolvents are ionic liquids (ILs), formed by a cation-anion pair and having a melting point below 100 °C [21]. In 2002, a series of compounds based on an imidazolium cation with different anions were employed for the dissolution of cellulose [22]. In subsequent works, the range of IL employed for this process has been considerably expanded [23–25].

The interaction of ionic liquids with the polymer chains of cellulose results in the rupture of the hydrogen and intermolecular bonds that are present in its macro molecules. The dissolution of cellulose in IL involves a number of stages: infiltration, limited swelling, partial dissolution, dissociation, and complete dissolution [26]. Based on nuclear magnetic resonance (NMR) data, it has been revealed that the solvation of cellulose in the IL [BMIm]Cl occurs through the formation of hydrogen bonds between hydroxyl protons of the cellulose and the chloride ions that make up the IL [27]. Structural changes of microcrystalline cellulose (MCC) during its dissolution in [EMIm][OAc] over a wide concentration range (0 – 100 %) were investigated using small-angle X-ray scattering (SAXS) [28]. It was shown that at a cellulose content of about 35 % (mol) in solution, a cellulose/IL complex with high structural periodicity is formed, and a crystalline structure is observed at a concentration exceeding 40 % (mol). In addition to the study of solubility, an equally important issue is the study of the morphology of regenerated cellulose after its isolation from IL solutions [25, 29]. Previously, we published the results of studies of the structure of cellulose fibers obtained by extrusion of its solutions in [BMIm]Cl into water [30]. It was found that the fibers consist of a core consisting of pseudofibrils about 30 nm thick, and a shell. At the same time, the tensile strength averaged 250 MPa.

The aim of this work was to study the morphological features and thermal stability of wood cellulose LS-0, depending on its concentration in solutions based on the ionic liquid [BMIm]Cl.

## 2. Materials and methods

The ionic liquid 1-Butyl-3-methylimidazolium chloride [BMIm]Cl was prepared according to the procedure given previously [30].

FT-IR spectrum was recorded on a Bruker Tensor 27 spectrometer equipped with an ATR attachment (Pike MIRacle) with a germanium (Ge) crystal in the frequency range 800 – 4000 cm<sup>-1</sup> with 32 rescans and 4 cm<sup>-1</sup> resolution.

Thermogravimetric analysis (TGA) of cellulose samples was conducted on thermoanalytical scales TG 209 F1, manufactured by the Netzsch company, in an inert argon environment at a heating rate of 20 °C/min. The samples were suspended at a weight of 3 – 6 mg. The data were analyzed using the NETZSCH Proteus program (version 4.8.4).

X-ray radiographs (XRD) of cellulose samples were obtained at room temperature on a Rigaku Smartlab SE automated diffractometer using Cu K $\alpha$  radiation with a wavelength of 1.5406 Å (Bragg reflection geometry, 40 kV, 50 mA). The  $2\theta$  angle range was set to 10 – 50°, with a scanning step of 0.02° and a scanning speed of 5 °/min.

The electron microscopy analysis was made using a JSM 7500F scanning electron microscope (JEOL, Japan). The spatial resolution varied between 1.0 nm (15 kV of accelerating voltage) and 1.4 nm (1 kV).

Bleached wood sulfate pulp from a mixture of hardwoods (LS-0 grade, GOST 28172-89, manufacturer – JSC “Arkhangelsk PPM”, DP 900) was washed with water, filtered and dried at 55 °C to constant weight. 1-Methylimidazole (99 %, Acros Organics), 1-chlorobutane (99 %, Acros Organics). Methylene chloride and acetonitrile were purified by distillation and stored over 3 Å molecular sieves.

The preparation of samples of regenerated cellulose was conducted in accordance with the methodology outlined in reference [32]. A fixed quantity of wood cellulose (LS-0) was introduced into [BMIm]Cl solutions of varying concentrations (98, 92, 86, 80, and 74 %). Subsequently, the samples were heated at 65 – 70 °C to remove the acetonitrile. Once the solvent had been completely removed, the impregnated [BMIm]Cl was heated to 110 °C for a period of two hours. Solutions with LS-0 concentrations of 2, 8, 14, 20, and 26 % were obtained. Following a period of cooling to room temperature, 20 mL of distilled water was added to the resulting samples. After four hours, the water was drained off the precipitated cellulose, and 20 mL of water was added to the precipitate. This washing process was repeated five more times in order to completely remove the [BMIm]Cl. The regenerated cellulose was then dried at 55 °C until it reached a constant weight.

## 3. Results and discussion

### 3.1. Effect of dissolution of wood cellulose in [BMIm]Cl on its structure

The use of ionic liquids as a solvent for cellulose, discovered by Swatoski et al. [22], has gained widespread acceptance. In subsequent studies, a wide range of such compounds was investigated, in which the key elements are quaternized ammonium or phosphonium cations, and organic and inorganic acids are used as anions [25]. However, not all of them demonstrated satisfactory cellulose dissolving capacity. In addition to the structure of the IL, the degree of polymerization of the cellulose itself also influences the production of a homogeneous solution. Dissolution of microcrystalline cellulose (MCC), which is characterized by low DP, is the most effective. In this case, it is possible to obtain solutions with a high concentration, up to 20 %, using IL [BMIm]Cl [31]. In the previous work [32], devoted to the study of the dissolution of wood cellulose LS-0 in IL based on [BMIm]<sup>+</sup> with various anions, it was established that homogeneous solutions of LS-0 with a concentration of up to 8 % (wt.) are formed when using the Cl<sup>-</sup> anion. When the anion is replaced by Br<sup>-</sup> or CH<sub>3</sub>C(O)O<sup>-</sup>, the dissolution of LS-0 is significantly reduced, and the maximum concentration is 2 and 4 % (wt.),

respectively. It was also found that the imidazolium cation in [BMIm]OAc reacts with the aldehyde group of the open end of the carbohydrate chain. Therefore, our further studies aimed at dissolving cellulose LS-0 in IL were carried out using [BMIm]Cl.

For our study, LS-0 solutions in [BMIm]Cl with concentrations of 2, 8, 14, 20, and 26 % were prepared. After precipitation of LS-0 in water and subsequent removal of [BMIm]Cl from the cellulose matrix, the hydrogen bonds that were disrupted during dissolution are formed (Fig. 1).

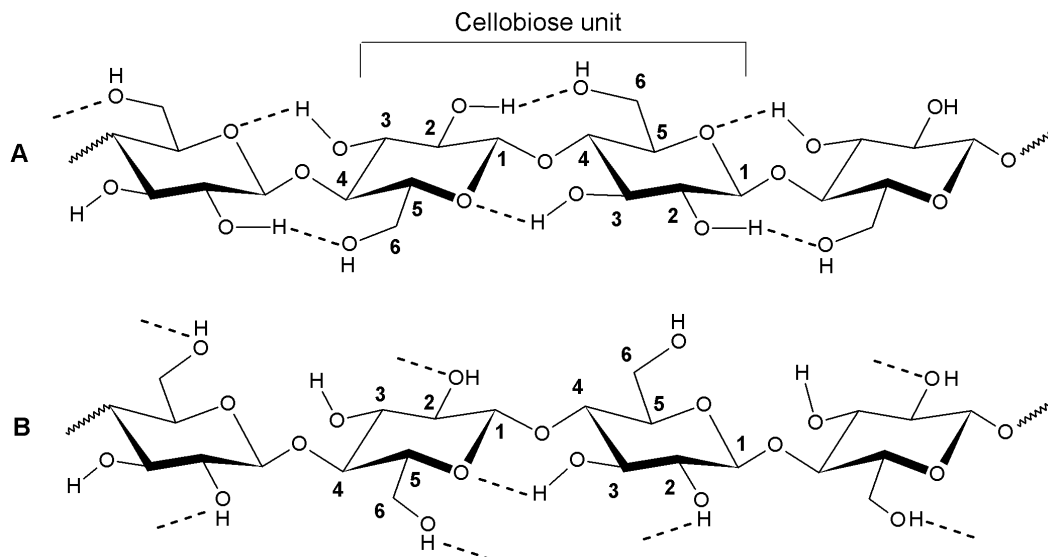


FIG. 1. Cellulose polymer chain and hydrogen bonds in the original cellulose (A) and in the regenerated cellulose (B) obtained by precipitation from its solutions in ionic liquid

Figure 1(A) illustrates that natural cellulose predominantly comprises intramolecular hydrogen bonds situated at the cellobiose unit [6, 7]. In the process of dissolution in IL, these bonds are disrupted as a result of the interaction between the hydroxyl groups and [BMIm]Cl. As the concentration of LS-0 in the IL increases, the efficiency of its dissolution is reduced. This is due to the insufficient quantity of IL capable to interact with hydroxyl groups. In this instance, a certain degree of initial ordering in the crystalline regions of the cellulose may be retained due to the retention of hydrogen bonds in the cellobiose unit. After treating the cellulose solution in IL with water, the solvent is removed, which leads to the formation of new intermolecular hydrogen bonds within the polymer (Fig. 1(B)). As a result, the cellulose molecules become more tightly packed and strongly bonded to each other. In some cases, such packaging reduces its reactivity, similar to what happens with cellulose II [6, 7]. This phenomenon was observed during the precipitation of LS-0 cellulose in water from its solutions in [BMIm]Cl with a concentration of up to 6 % [32].

Figure 2 illustrates the X-ray diffraction patterns of LS-0 cellulose solutions in [BMIm]Cl.

As evidenced by the provided diffractograms, the initial LS-0 sample exhibits the presence of crystalline formations [33]. The crystallinity is markedly diminished in [BMIm]Cl solutions. Nevertheless, the diffractograms do reveal

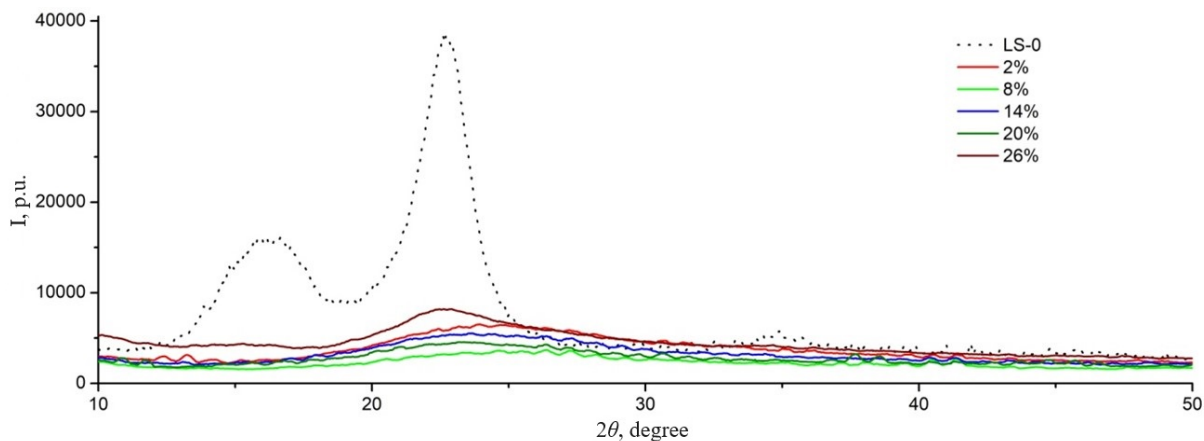


FIG. 2. Diffractograms of LS-0 cellulose solutions and its solutions in [BMIm]Cl. LS-0 content: 2, 8, 14, 20 and 26 %

the presence of weakly pronounced peaks, which can be taken to indicate the existence of a residual amount of ordered regions. This phenomenon is particularly evident at a concentration of 26 %. These ordered regions probably play a key role in the restoration of the structural features of cellulose during its precipitation in water upon removal of the IL. As a result of this process, structures are formed that resemble the original cellulose in their architecture. Fig. 3 shows scanning electron microscopy (SEM) images of recovered cellulose samples obtained from its solutions in [Bmim]Cl.

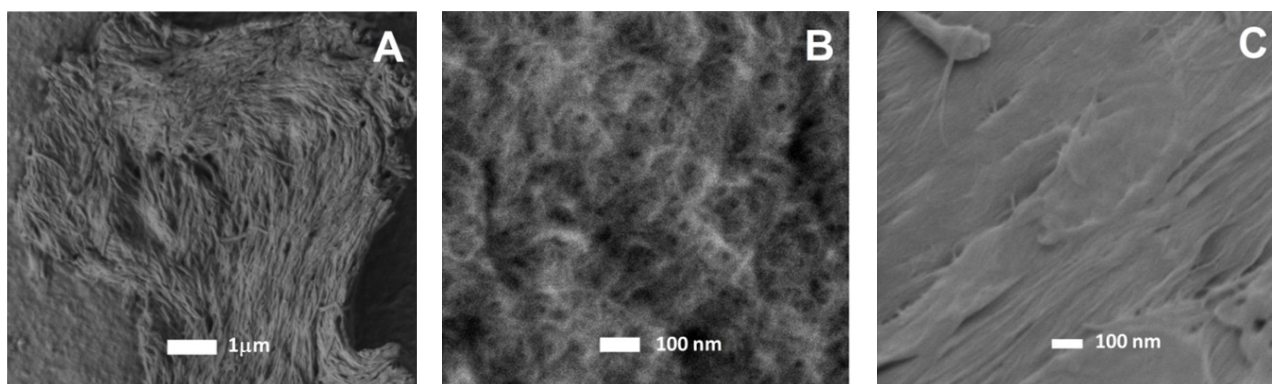


FIG. 3. SEM-image of precipitated (recovered) cellulose from its solutions in [Bmim]Cl: (1) fragment of precipitated cellulose 26 %, (2) film surface 2 %, (3) film surface 5 %

Scanning electron microscopy images (Fig. 3(A)) demonstrate that at high concentrations of LC-0 in [Bmim]Cl and its subsequent precipitation, the main structural fragments of cellulose are preserved. In this case, partial swelling of the fibrils occurs, while their morphological characteristics remain unchanged. This indicates that hydrogen bonds in the cellobiose units are practically unaffected. At a low concentration of cellulose, the dissolution process is particularly intense, which leads to the formation of transparent solutions. In this case, cellulose deposited on a glass substrate exhibits individual nanoscale fragments (Fig. 3(A,B)).

### 3.2. IR spectroscopy

Changes in the structural features of regenerated cellulose are clearly observed when analyzed using IR spectroscopy (Fig. 4).

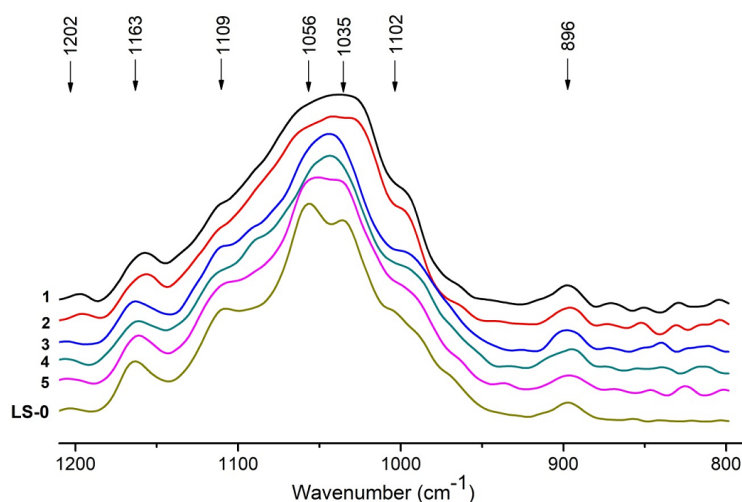


FIG. 4. IR spectra of precipitated wood cellulose LS-0 after dissolution in [BMIm]Cl. The percentages in IL: 1 – 2 %, 2 – 8 %, 3 – 14 %, 4 – 20 %, 5 – 26 %, and LS-0 is the original cellulose (wave numbers are given for the original cellulose LS-0)

Figure 3 illustrates the spectral characteristics of the initial LS-0 and those observed following a dissolution/precipitation cycle in water from its solutions in [BMIm]Cl with a concentration of 2 – 26 % (weight). The portion of the spectrum depicted in Fig. 3 pertains to the valence vibration region of the structural units constituting the cellobiose linkage. The band assignment of the IR spectrum of cellulose was conducted in accordance with the data presented in the sources cited in the references [34, 35]. It can be observed that in solutions with concentrations of 2 and 8 %, a notable amorphization of LS-0 occurs, as evidenced by the disappearance of the bands at 1056 and 1035  $\text{cm}^{-1}$ . These bands, which refer to

the valence vibrations of C–O (mainly C(3)–O(3)H) and deformation vibrations of C–O groups in the primary alcohol, respectively, are absent in the amorphous state. As the concentration of LS-0 in [BMIm]Cl increases, the bands in question become more pronounced. At a concentration of 26 %, two characteristic maxima are observed, which are typical of the original cellulose. A notable alteration in the regenerated LS-0's morphology is indicated by the broadening of the band at 1109  $\text{cm}^{-1}$ , which belongs to the asymmetric vibrations of the glucopyranose ring. Concurrently, the band at 1163  $\text{cm}^{-1}$  (asymmetric vibrations of the  $\beta$ -glycosidic C–O–C bond) undergoes a shift of 5  $\text{cm}^{-1}$ , which is particularly pronounced for low concentrations (Fig. 3). There is also an increase in the intensity of the weak band at 1202  $\text{cm}^{-1}$ , corresponding to in-plane deformation vibrations of OH groups. Although this band has insignificant intensity in the spectrum of LS-0 itself, the increase in its intensity indicates an increase in the content of alcohol groups that do not have hydrogen bonds with neighboring hydroxyls. On the other hand, the 896  $\text{cm}^{-1}$  band corresponding to the valence vibrations of the  $\beta$ -glycosidic C–O–C bond undergoes the least changes. Thus, the results of vibrational spectroscopy indicate significant changes occurring in the structure of LS-0 cellulose during dissolution in [BMIm]Cl and during its subsequent precipitation in water.

### 3.3. Thermal stability of regenerated cellulose

The thermal stability of cellulose is a characteristic that can be employed in the prediction of the stability of products subjected to temperature exposure. As demonstrated in reference [36], the thermochemical conversion of cellulose is contingent upon its associated components, namely hemicelluloses. Thermal stability of regenerated cellulose may also depend on the type of solvents used during its processing [37]. Regenerated celluloses obtained from their solutions in ionic liquids also show differences in TG analysis conditions. Using the example of microcrystalline celluloses dissolved in ionic liquids of different chemical compositions, it was found that the nature of the solvent affects both the crystallinity and the thermal stability of the recovered cellulose [38, 39].

In contrast to MCC, the wood cellulose LS-0 used in this work has a higher DP and contains both crystalline and amorphous regions in its composition. The thermal stability of the obtained regenerated cellulose samples was investigated using TGA. Fig. 5 shows the TG and DTG curves of wood pulp samples isolated from its solutions in [BMIm]Cl ionic liquid.

Figure 5 illustrates that all samples exhibit a slight mass loss in the low-temperature region (less than 100 °C) due to the evaporation of absorbed water. In the temperature range above 200 °C, there are notable differences in the behavior of TGA curves, as evidenced by the alteration in the maximum values of DTG curves and the values of the final residual mass (Fig. 5, Table 1).

TABLE 1. TGA/DTG results of cellulose samples before and after dissolution in [BMIm]Cl (LS-0 content in IL, 2 %; C – 8 %; D – 14 %; E – 20 %; F – 26 %)

Sample ( %, wt)	$T_{\text{mrd1}}$ (°C)	$T_{\text{mrd2}}$ (°C)	Coke residue ( %)
LS-0	290	348.3	9.5
2	— / —	318.7	20.7
8	— / —	333.4	18.3
14	291.9	358.7	15.7
20	284.8	352.5	14.0
26	297.0	364.2	12.6

$T_{\text{mrd1}}$  and  $T_{\text{mrd2}}$  – temperature of maximum decomposition rate at the first (1) and second (2) stages on the DTG curve

As evidenced by the data presented in Table 1, the temperature of maximum decomposition rate ( $T_{\text{mrd2}}$ ) of the original pulp is 348.3 °C, and the value of coke residue is 9.54 %. In the case of regenerated pulp samples, these parameters exhibit a markedly different profile. A decrease in the value of  $T_{\text{mrd2}}$  is observed in the case of LS-0 in [BMIm]Cl 2 and 8 % compared to the original cellulose. As the concentration increases, two well-defined temperature maxima are observed in the DTG curves. Concurrently, the  $T_{\text{mrd1}}$  value for LS-0 and all samples derived from ILs remains essentially unaltered, whereas  $T_{\text{mrd2}}$  shifts towards the high-temperature region. Additionally, a notable increase in coke residue is observed when the concentration of cellulose in [BMIm]Cl is reduced. This phenomenon can be attributed to alterations in the intermolecular interactions of cellulose chains. Apparently, the content of a large number of ordered structures (crystallites) in the original cellulose at the initial stage of thermal destruction can contribute to the acceleration of dehydration processes and the breakdown of glycosidic bonds (Fig. 1(A)). This leads to the formation of both volatile

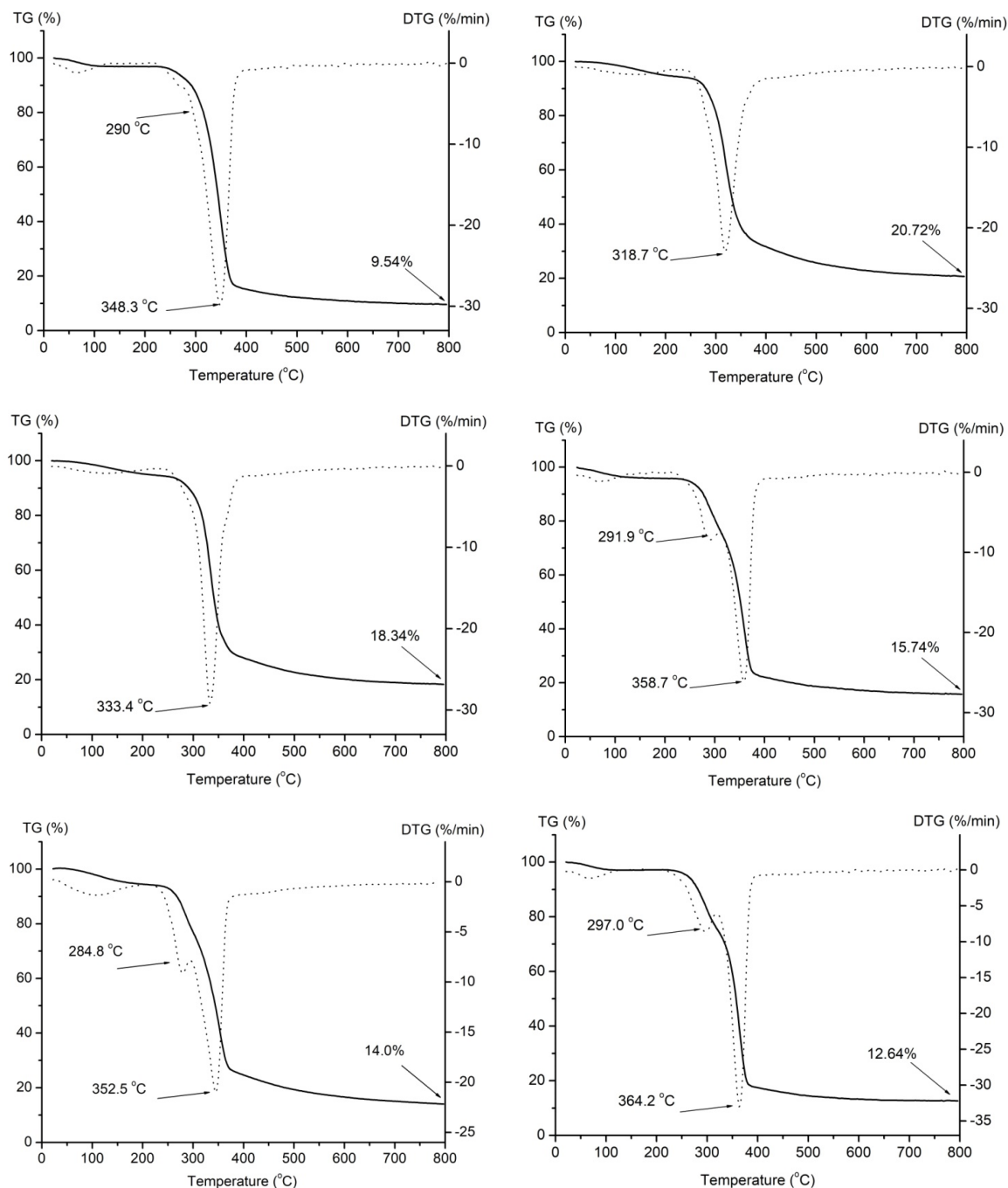


FIG. 5. TG/DTG analysis of LS-0 samples after dissolution in [BMIm]Cl: A – initial LS-0; B – 2 %; C – 8 %; D – 14 %; E – 20 %; F – 26 %

furan derivatives and levoglucosan [40], as well as solid products – unsaturated polyene structures capable of crosslinking and aromatization (coke formation) [41].

Similarly, coke residue is also formed in amorphous regions of cellulose with less ordered structures (Fig. 1(B)). Fig. 6 depicts a plot of the formal dependence of coke residue formation on the concentration of cellulose in [BMIm]Cl.

As illustrated in Fig. 6, an increase in LS-0 concentration within the ionic liquid is associated with a reduction in coke residue within the regenerated cellulose samples. At the same time, the rate of formation of volatile products is observed to increase, as evidenced by a decline in  $T_{\text{mrd}2}$  (Table 1). This phenomenon may be attributed to the complete destruction of the initial hydrogen-bonded structure at concentrations up to 8 %. After removal of the ionic liquid, cellulose undergoes chaotic restoration of hydrogen bonds, which leads to its amorphization. As the concentration of cellulose in [BMIm]Cl increases, the dissolution process becomes more difficult, which contributes to the partial preservation of crystalline regions. It can be assumed that after precipitation in water and removal of IL from cellulose, pseudofibrils are formed on the basis of partially ordered fragments [30]. The listed circumstances allow us to assume that the thermal destruction of

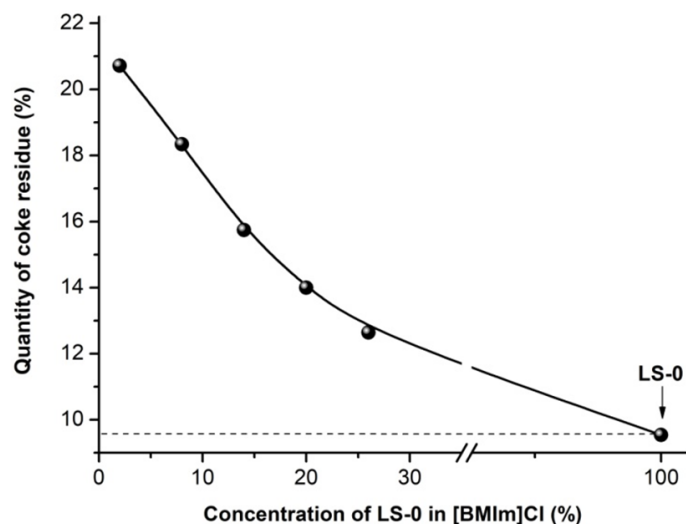


FIG. 6. Dependence of coke residue formation on the concentration of LS-0 in [BMIm]Cl

cellulose depends on the amorphous and an ordered region contained in its structure and is determined by the difference in the directions of thermochemical processes (Fig. 7).

As shown in Fig. 7, the initial stage of thermal destruction of cellulose includes the elimination of water molecules and the formation of unsaturated C=C bonds. However, further development of the process begins to depend on the morphological features of cellulose. Apparently, the ordering of the crystalline regions caused by hydrogen bonds in the glycoside unit (Fig. 1(A)) significantly reduces the mobility of cellulose chains. Therefore, stabilization of dehydroxylated hexoses of the cellobiose unit occurs due to the rupture of the glycoside bond (Fig. 7(A)). As a result, unstable structural fragments capable of forming low-molecular compounds are formed at the site of the rupture. After dissolution in the IL with subsequent regeneration, the morphology of cellulose changes (Fig. 1(B)), which is reflected in the process of its thermal destruction (Fig. 5(B, C) and Fig. 7(B)). In regenerated cellulose, especially at low concentrations in the IL, the hydrogen bonds that determine its spatial structure are destroyed. When cellulose is precipitated with water from an IL solution, new hydrogen bonds are chaotically formed between its macromolecules, the arrangement of which differs from the initial contacts. This leads to a change in the morphology of cellulose. In this case, as for the original LS-0, the initial act is the elimination of water. However, at a later stage, the thermochemical processes begin to differ. Since macromolecules in amorphous regions can have increased mobility, the stabilization of dehydroxylated hexoses can lead

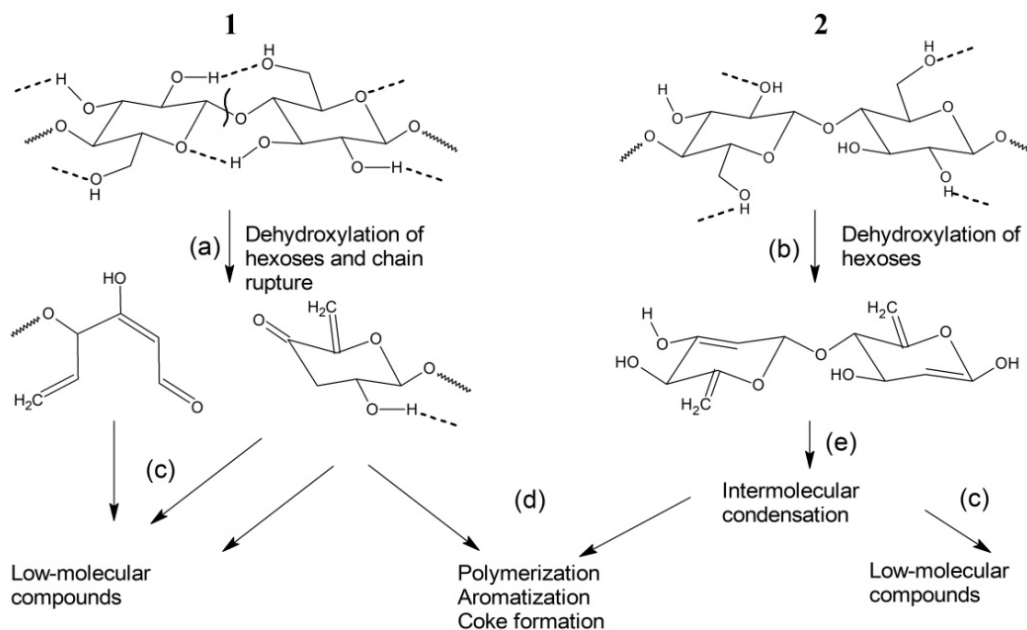


FIG. 7. Formal representation of thermal degradation of regenerated LS-0 cellulose before (1) and after dissolution in [BMIm]Cl (2)

to intermolecular reactions with the formation of polyene structures. In this case, the rupture of glycosidic bonds and the formation of low molecular weight pyrolysis products occur to a lesser extent, which leads to significant formation of coke residue (Fig. 5). As the LS-0 content in ILs increases, the crystallinity disorder decreases, which also affects the change in the directions of thermochemical processes. In this case, the process of formation of low molecular weight fragments accelerates, which, in turn, leads to a decrease in the amount of polyene structures and coke residue.

Figure 8 depicts the diffractograms of the regenerated cellulose samples. It can be observed that at concentrations of 2 and 8 %, the disappearance of characteristic reflections at  $2\theta$  (16.2 and 22.7) occurs, which may indicate the complete disappearance of the original ordering. This phenomenon is reflected in the thermochemical processes observed in the TGA curves (Fig. 5(B, C)).

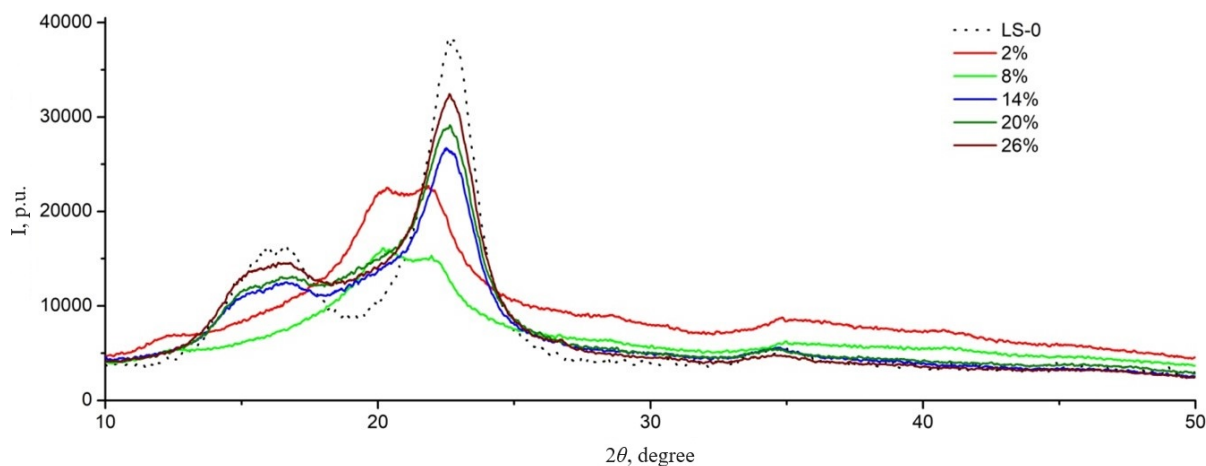


FIG. 8. Diffractograms of regenerated cellulose samples

As illustrated in Fig. 5(D), the thermal decomposition of cellulose regenerated from the solution containing 14 % is significantly different from the previous cases. The amount of carbon residue decreases, and two characteristic maxima appear in the DTG curve:  $T_{\text{mrd1}}$  (291.9 °C) and  $T_{\text{mrd2}}$  (358.7 °C). It is noteworthy that the DTG curve of the original LS-0 cellulose (Fig. 5(A)) also shows a weak peak in the range of 290 °C, which is difficult to distinguish from the primary peak of  $T_{\text{mrd2}}$ .

It can be assumed that this peak is also present in samples B and C (Fig. 5), although less distinct than that observed for  $T_{\text{mrd2}}$ . The same thermal degradation pattern is evident in the samples prepared from 20 and 26 % solutions (Fig. 5(E, F)). The maxima observed for  $T_{\text{mrd1}}$  and  $T_{\text{mrd2}}$  in the DTG curves can be explained by the presence of two structurally different phases contained in the samples. The presence of these peaks can be explained by the incomplete dissolution of the ordered regions present in the cellulose fibers.

Apparently, the initial dissolution of LS-0 cellulose involves the interaction of [BMIm]Cl with the most accessible amorphous regions, which leads to the consumption of most of the IL. The observation of crystalline formations with an ordered structure indicates a reduced susceptibility to dissolution, which suggests that their original structure is partially preserved. During precipitation of cellulose in an aqueous medium, a rapid regeneration of amorphous regions occurs, and the presence of partially ordered structures leads to the formation of pseudofibrils. In light of these observations, the first maximum observed in the range of  $290 \pm 7$  °C in the DTG curves can be attributed to the decomposition of the amorphous phase, and the second maximum to structural fragments with partial order.

The application of X-ray diffraction analysis (Fig. 8) to the examination of reduced cellulose samples enables the clear verification of structural alterations affecting the alteration of thermal stability. The graph illustrates the presence of ordered structures in the samples.

The degree of crystallinity was evaluated in accordance with the peak height method of the diffractogram, as previously described in the literature [42]. The following formula may be employed:

$$C = 100 \cdot \frac{I_{200} - I_{\text{non-cr}}}{I_{200}},$$

where  $C$  – degree of crystallinity [%], and  $I_{200}$  is the maximum peak intensity at the angle  $2\theta$  equal to 22 – 24 degrees. Additionally,  $I_{\text{non-cr}}$  represents the diffraction intensity of the non-crystalline part, which is taken at the angle  $2\theta$  equal to 18 degrees between the peaks. The results calculated using this formula are presented in Table 2.

Thus, the conducted studies of regenerated cellulose LS-0, obtained by precipitation from its solutions in [BMIm]Cl, show that there is a significant transformation of its structure. This is clearly observed during analysis using IR spectroscopy. These changes are fully observed in the results of TG analysis, which is expressed in a change of its thermal stability. Moreover, for high concentrations, this parameter increases.

TABLE 2. Degree of crystallinity of the regenerated cellulose under study

Sample	Degree of crystallinity C ( % )
Initial cellulose LS-0	81.3
LS-0 2 % after dissolution in [BMIm]Cl	41.8
LS-0 8 % after dissolution in [BMIm]Cl	43.7
LS-0 14 % after dissolution in [BMIm]Cl	59.7
LS-0 20 % after dissolution in [BMIm]Cl	59.3
LS-0 26 % after dissolution in [BMIm]Cl	62.7

#### 4. Conclusions

The study examined the physicochemical properties and morphological features of regenerated cellulose obtained by precipitation in water from its solutions in [BMIm]Cl with concentrations from 2 to 26 %. It was found that when the cellulose content in [BMIm]Cl was up to 8 %, significant morphological changes occurred, expressed in a significant change in its infrared spectra and a decrease in thermal stability. With increasing concentration, the spectral characteristics of the reconstituted cellulose approach the original LS-0. At the same time, the thermal stability increases significantly, and at LS-0 concentration of 26 %, the temperature of maximum decomposition rate exceeds this parameter for pure cellulose by more than 15 degrees. Thus, the study revealed significant changes in the structure of cellulose fibers that occur during their dissolution in ionic liquid [BMIm]Cl and determine the physicochemical properties of the reconstituted cellulose.

#### References

- [1] Szabó L., Milotskyi R., Sharma G., K. Takahashi. Cellulose processing in ionic liquids from a materials science perspective: turning a versatile biopolymer into the cornerstone of our sustainable future. *Green Chem.*, 2023, **25**, P. 5338-5389.
- [2] Gharekhani S., Sadeghinezhad E., Kazi S.N., Yarmand H., Badarudin A., Safaei M.R., Zubir M.N.M. Basic effects of pulp refining on fiber properties – a review. *Carbohydr. Polym.*, 2015, **115**, P. 785–803.
- [3] Stovbun S.V., Lomakin S.M., Shchegolikhin A.I., et al. Role of Structural Stresses in the Thermodestruction of Supercoiled Cellulose Macromolecules after Nitration. *Russ. J. Phys. Chem. B*, 2018, **12**, P. 36–45.
- [4] Stovbun S.V., Mikhaleva M.G., Skoblin A.A., Usachev S.V., Nikolsky S.N., Kharitonov V.A., Zlenko D.V., et al. Zhurkov's stress-driven fracture as a driving force of the microcrystalline cellulose formation. *Polymers*, 2020, **12** (12), 2952.
- [5] Cabiac A., Guillon E., Chambon F., Pinel C., Rataboul F., Essayem N. Cellulose reactivity and glycosidic bond cleavage in aqueous phase by catalytic and non catalytic transformations. *Appl. Catal. A*, 2011, **402**, P. 1–10.
- [6] Heinze T. Cellulose: Structure and Properties. In: Rojas, O. (eds) Cellulose Chemistry and Properties: Fibers, Nanocelluloses and Advanced Materials. *Advances in Polymer Science*, 2015, **271**, Springer, Cham.
- [7] Kondo T. Hydrogen bonds in cellulose and cellulose derivatives. In: Dumitriu S. (ed) *Polysaccharides: structural diversity and functional versatility*, 2nd edn. Marcel Dekker, New York, 2005, P. 69–98.
- [8] Stovbun S.V., Nikol'skii S.N., Mel'nikov V.P., et al. Chemical physics of cellulose nitration. *Russ. J. Phys. Chem. B*, 2016, **10**, P. 245–259.
- [9] Anpilova A.Y., Mastalygina E.E., Khrameeva N.P., et al. Methods for Cellulose Modification in the Development of Polymeric Composite Materials (Review). *Russ. J. Phys. Chem. B*, 2020, **14**, P. 176–182.
- [10] Morris E., Pulham C.R., Morrison C.A. Structure and properties of nitrocellulose: approaching 200 years of research. *RSC Adv.*, 2023, **13**, P. 32321–32333.
- [11] Sayyed A.J., Deshmukh N.A., Pinjari D.V. A critical review of manufacturing processes used in regenerated cellulosic fibres: viscose, cellulose acetate, cuprammonium, LiCl/DMAc, ionic liquids, and NMMO based lyocell. *Cellulose*, 2019, **26**, P. 2913–2940.
- [12] Burchard W., Habermann N., Klüfers P., Seger B., Wilhelm U. Cellulose in Schweizer's Reagent: A Stable, Polymeric Metal Complex with High Chain Stiffness. *Angew. Chem. Int. Ed.*, 1994, **33**, P. 884–887.
- [13] Dawsey T.R., McCormick C.L. The lithium chloride/dimethylacetamide solvent for cellulose: a literature review. *J. Macromol. Sci. Polymer. Rev.*, 1990, **30** (3-4), P. 405–440.
- [14] Xu A., Wang J., Wang H. Effects of anionic structure and lithium salts addition on the dissolution of cellulose in 1-butyl-3-methylimidazolium-based ionic liquid solvent systems. *Green Chem.*, 2010, **12**, P. 268–275.
- [15] Heinze T., Koschella A. Solvents applied in the field of cellulose chemistry – A mini review. *Polímeros: Ciência e Tecnologia*, 2005, **15**, P. 84–90.
- [16] Huang Y., Xin P., Li J., Shao Y., Huang C., Pan H. Room-temperature dissolution and mechanistic investigation of cellulose in a tetra-butylammonium acetate/dimethylsulfoxide system. *ACS Sustain. Chem. Eng.*, 2016, **4** (4), P. 2286–2294.
- [17] Kostag M., Jedvert K., Ahtel C., Heinze T., El Seoud O.A. Recent Advances in Solvents for the Dissolution, Shaping and Derivatization of Cellulose: Quaternary Ammonium Electrolytes and their Solutions in Water and Molecular Solvents. *Molecules*, 2018, **23**, 511.
- [18] El Seoud O.A., Kostag M., Jedvert K., Malek N.I. Cellulose in Ionic Liquids and Alkaline Solutions: Advances in the Mechanisms of Biopolymer Dissolution and Regeneration. *Polymers*, 2019, **11**, 1917.
- [19] Olsson C., Hedlund A., Idström A., Westman G. Effect of methylimidazole on cellulose/ionic liquid solutions and regenerated material therefrom. *J. Mater. Sci.*, 2014, **49**, P. 3423–3433.
- [20] Graenacher C. Cellulose solution. US Patent, 1934 (p. 1934176 A). Graenacher C., Sallmann R. Cellulose solution and process of making same. US Patent, 1939 (p. 2179181 A).
- [21] Ghandi K. A Review of Ionic Liquids, Their Limits and Applications. *Green and Sustainable Chemistry*, 2014, **4** (1), P. 44–53.

- [22] Swatloski R.P., Spear S.K., Holbrey J.D., Rogers R.D. Dissolution of Cellulose with Ionic Liquids. *J. Am. Chem. Soc.*, 2002, **124** (18), P. 4974–4975.
- [23] Fukaya Y., Sugimoto A., Ohno H. Superior solubility of polysaccharides in low viscosity, polar, and halogen-free 1,3-dialkylimidazolium formates. *Biomacromol.*, 2006, **7**, P. 3295–3297.
- [24] Xu A., Zhang Y., Lu W., Yao K., Xu H. Effect of alkyl chain length in anion on dissolution of cellulose in 1-butyl-3-methylimidazolium carboxylate ionic liquids. *J. Mol. Liq.*, 2014, **197**, P. 211–214.
- [25] Gupta K.M., Jiang J. Cellulose dissolution and regeneration in ionic liquids: A computational perspective. *Chemical Engineering Science*, 2015, **121**, P. 180–189.
- [26] Li X.J., Sun Y.S., Zhao Q. Experimental Research on the Solubility of Cellulose in Different Ionic Liquids. *Adv. Mat. Res.*, 2013, (**690-693**), P. 1568–1571.
- [27] Remsing R.C., Swatloski R.P., Rogers R.D., Moyna G. Mechanism of cellulose dissolution in the ionic liquid 1-n-butyl-3-methylimidazolium chloride: a <sup>13</sup>C and <sup>35/37</sup>Cl NMR relaxation study on model systems. *Chem. Commun. (Camb.)*, 2006, **12**, 1271–3.
- [28] Endo T., Hosomi S., Fujii S., Ninomiya K., Takahashi K. Nano-Structural Investigation on Cellulose Highly Dissolved in Ionic Liquid: A Small Angle X-ray Scattering Study. *Molecules*, 2017, **22**, 178.
- [29] Medronho B., Lindman B. Brief overview on cellulose dissolution/regeneration interactions and mechanisms. *Advances in colloid and interface science*, 2015, **222**, P. 502–508.
- [30] Usachev S.V., Zlenko D.V., Nagornova I.V., Koverzanova E.V., Mikhaleva M.G., Vedenkin A.S., Vtyurina D.N., Skoblin A.A., Nikolsky S.N., Politenkova G.G., Stovbun S.V. Structure and properties of helical fibers spun from cellulose solutions in (Bmim)Cl. *Carbohydr. Polym.*, 2020, **235**, 11586.
- [31] Pinkert A., Marsh K.N., Pang S., Staiger M.P. Ionic liquids and their interaction with cellulose. *Chem. Rev.*, 2009, **109** (12), P. 6712–6728.
- [32] Mikhaleva M., Vedenkin A., Usachev S., Levina I. Dissolution Efficiency of Wood Pulp in Ionic Liquids Based on 1-Butyl-3-Methylimidazolium with Different Anions. *Russ. J. Phys. Chem. B*, 2023, **17**, P. 996–1004.
- [33] Man Z., Muhammad N., Sarwono A., et al. Preparation of Cellulose Nanocrystals Using an Ionic Liquid. *J. Polym. Environ.*, 2011, **19**, P. 726–731.
- [34] Široký J., Blackburn R., Bechtold T., Taylor J., White P. Attenuated total reflectance Fourier-transform infrared spectroscopy analysis of crystallinity changes in lyocell following continuous treatment with sodium hydroxide. *Cellulose*, 2010, **17** (1), P. 103–115.
- [35] Haulea L.V., Carr C.M., Rigout M. Investigation into the supramolecular properties of fibres regenerated from cotton based waste garments. *Carbohydr. Polym.*, 2016, **144**, P. 131–139.
- [36] Wang J., Minami E., Kawamoto H. Thermal reactivity of hemicellulose and cellulose in cedar and beech wood cell walls. *J. Wood. Sci.*, 2020, **66**, 41.
- [37] Rebière J., Heuls M., Castignolles P., Violleau F., Durrieu V. Structural modifications of cellulose samples after dissolution into various solvent systems. *Anal. Bioanal. Chem.*, 2016, **408**, P. 8403–8414.
- [38] Im J., Lee S.H., Insol J., Won K.J., Kim K.S. Structural characteristics and thermal properties of regenerated cellulose, hemicellulose and lignin after being dissolved in ionic liquids. *J. Indus. Engin. Chem.*, 2022, **107**, P. 365–375.
- [39] Yang H., Jiang J., Zhang B., Zhang W., Xie W., Li J. Experimental study on pretreatment effects of [BMIM]HSO<sub>4</sub>/ethanol on the thermal behavior of cellulose. *RSC Adv.*, 2022, **12**, 10366.
- [40] Shen D.K., Gu S. The mechanism for thermal decomposition of cellulose and its main products. *Bioresource Technology*, 2009, **100**, P. 6496–6504.
- [41] Perova A.N., Brevnov P.N., Usachev S.V., et al. Comparative Analysis of Thermal and Physico-Mechanical Properties of Polyethylene Compositions Containing Microcrystalline and Nanofibrillary Cellulose. *Russ. J. Phys. Chem. B*, 2021, **15**, P. 716–723.
- [42] Terinte N., Ibbett R., Schuster K.C. Overview on native cellulose and microcrystalline cellulose I structure studied by X-ray diffraction (WAXD): Comparison between measurement techniques. *Lenzinger Berichte*, 2011, **89** (1), P. 118–131.

---

*Submitted 2025; revised 2025; accepted 2025*

#### *Information about the authors:*

*Mariya G. Mikhaleva* – Ph.D, senior researcher N.N. Semenov Federal Research Center for Chemical Physics Russian Academy of Sciences, 4 Kosygina Street, Moscow, Russian Federation 119991; ORCID 0000-0001-8192-69292; maria.mikhaleva@chph.ras.ru

*Sergey V. Usachev* – Ph.D, senior researcher N.N. Semenov Federal Research Center for Chemical Physics Russian Academy of Sciences, 4 Kosygina Street, Moscow, Russian Federation 119991; ORCID: 0000-0002-8971-9358; usachevsv@inbox.ru

*Alexander S. Vedenkin* – researcher N.N. Semenov Federal Research Center for Chemical Physics Russian Academy of Sciences, 4 Kosygina Street, Moscow, Russian Federation 119991; ORCID 0000-0001-9295-583X; alexander.vedenkin@chph.ras.ru

*Mariya I. Ikim M.* – Ph.D, senior researcher N.N. Semenov Federal Research Center for Chemical Physics Russian Academy of Sciences, 4 Kosygina Street, Moscow, Russian Federation 119991; ORCID 0000-0003-4411-1119; maria.ikim@chph.ras.ru

*Galina G. Politenkova* – researcher N.N. Semenov Federal Research Center for Chemical Physics Russian Academy of Sciences, 4 Kosygina Street, Moscow, Russian Federation 119991, +7(495)939-7225; galina.politenkova@chph.ras.ru

*Sergey M. Lomakin* – Ph.D, head of laboratory Emanuel Institute of Biochemical Physics of Russian Academy of Sciences, 4 Kosygina Street, Moscow, Russian Federation 119991; ORCID 0000-0003-3191-8415; lomakin@sky.chph.ras.ru

*Conflict of interest:* the authors declare no conflict of interest.